Free Troposphere Ozone and Carbon Monoxide over the North Atlantic for 2001-2011

Aditya Kumar[1], Shiliang Wu[1, 2], Mark F. Weise[1*], Richard Honrath[1, #], R. Chris Owen[3], Detlev Helmig[4], Louisa Kramer[2], Maria Val Martin[5], Qinbin Li[6]

[1]Department of Civil & Environmental Engineering, Michigan Technological University, Houghton, Michigan, USA

[2]Department of Geological and Mining Engineering and Sciences, Michigan Technological University, Houghton, Michigan, USA

[*]Now at ARCADIS, Novi, Michigan, USA

[#]Deceased

[3]U.S. EPA, Research Triangle Park, North Carolina, USA

[4]Institute of Alpine and Arctic Research, University of Colorado at Boulder, Boulder, Colorado, USA

[5]Department of Atmospheric Sciences, Colorado State University, Fort Collins, Colorado, USA

[6]Department of Atmospheric & Oceanic Sciences, University of California Los Angeles, Los Angeles, California, USA

Abstract

In-situ measurements of carbon monoxide (CO) and ozone (O_3) at the Pico Mountain Observatory (PMO) located in the Azores, Portugal are analyzed together with results from atmospheric chemical transport modeling (GEOS-Chem) and satellite remote sensing (AIRS for CO and TES for O_3) to examine the evolution of free-troposphere CO and O_3 over the North Atlantic for 2001-2011. GEOS-Chem captured the seasonal cycles for CO and O_3 well but significantly underestimated the mixing ratios of CO, particularly in spring. Statistically significant (using a significance level of 0.05) decreasing trends were found for both CO and O_3 based on harmonic regression analysis of the measurement data. The best estimates of the possible trends for CO and O_3 measurements are -0.31 +/- 0.30 (2-σ) ppbv yr^{-1} and -0.21 +/- 0.11 (2-σ) ppbv yr^{-1} respectively. Similar decreasing trends for both species were obtained with GEOS-Chem simulation results. The major factor contributing to the reported possible decrease in CO and O_3 mixing ratios at PMO over the past decade is the decline in anthropogenic CO and O_3-precursor emissions in regions such as North America and Europe. The increase in Asian emissions does not seem to outweigh the impact of these declines resulting in overall decreasing trends for both CO and O_3. For O_3, however, increase in atmospheric water vapor content associated with climate change also appears to be a contributing factor causing enhanced destruction of the O_3 during transport from source regions. These hypotheses are supported by results from the GEOS-Chem tagged CO and tagged O_3 simulations.

1 Introduction

Carbon monoxide (CO) and ozone (O_3) are important atmospheric pollutants in the troposphere. The major sources of atmospheric CO include incomplete combustion of fossil fuels (*Holloway et al.*, 2000; *Khalil and Rasmussen*, 1994; *Seinfeld and Pandis*, 2006) and biomass burning. CO is also formed through the oxidation of volatile organic compounds (VOCs) by the hydroxyl radical (OH). O_3 is formed in the troposphere through photochemical reactions in the presence of O_3 precursors which include the nitrogen oxides ($NO + NO_2 = NO_x$), CO and VOCs. The dominant loss pathway for tropospheric O_3 is photolysis followed by reaction with water vapor.

Atmospheric transport across the North Atlantic Ocean carries air pollutants from the continent of North America towards Europe. CO has a chemical lifetime of several months (*Seinfeld and Pandis*, 2006) and the lifetime for O_3 is 2-4 weeks in the troposphere (*Law*, 2010). These relatively long lifetimes enable these species to undergo intercontinental transport. Thus, changes in emissions from source regions (such as North America) can have significant implications for atmospheric composition in downwind regions such as North Atlantic or Europe. *Li et al.* (2002) found that 20% of summer violations of O_3 air quality standards in Europe would not have occurred in the absence of North American anthropogenic emissions.

Increases in anthropogenic emissions of NO_x, CO and VOCs have led to increases in free tropospheric O_3 since pre-industrial times (*Wang et al.*, 1998) although several studies have reported divergent trends of tropospheric O_3 over different regions of the Northern Hemisphere (*Brunke et al.*, 1998; *Fusco and Logan*, 2003; *Guicherit and Roemer*, 2000; *Jaffe et al.*, 2003; *Lee et al.*, 1998; *Oltmans et al.*, 2006). Over the past decade, emissions of O_3

precursors have declined significantly in North America and Europe, while those in Asia have increased (*Hudman et al.*, 2009; *Vingarzan*, 2004). Figure 1 shows the trends of anthropogenic emissions of CO and NO_x in the United States (U.S.) from 2000-2011. U.S. sources account for approximately 80% of anthropogenic emissions from North America (*Wang et al.*, 2009). These changes in emissions are expected to influence the free troposphere CO and O_3 concentrations over the North Atlantic. The Pico Mountain Observatory located in the central North Atlantic region (details provided in the next section) is a unique site that can be used to measure species relevant to long range transport and thereby examine the direct continental outflow from North America. In this study, we combine analyses of the continuous in-situ measurements of CO and O_3 at this station and results from the Goddard Earth Observing System chemical (GEOS-Chem) transport model to examine the trends in free-tropospheric CO and O_3 over the North Atlantic for the past decade.

2 Measurement data

2.1 Measurements at the Pico Mountain Observatory

The Pico Mountain Observatory (PMO, formerly called PICO-NARE) is located on the summit of Pico Mountain on the Pico island in the Azores, Portugal (38° 28'N, 28° 24'W) at an altitude of 2225 m (*Honrath et al.*, 2004). This station is well above the Marine Boundary Layer (MBL) during summertime and ideal for examining the atmospheric composition of the lower free troposphere (FT). The island population is low (around 15,000) and is concentrated near sea level which results in the site having negligible anthropogenic influence on the free troposphere composition, although upslope flows have been found to occur resulting in the

transport of low-altitude air to the mountaintop (*Kleissl et al.*, 2007). However, the occurrence of such flow is not very frequent and even when it occurs it was found that the air did not originate from the surface (*Kleissl et al.*, 2007).

The station is also frequently impacted by export of North American pollution during summertime and outflow from arctic and subarctic regions resulting in transport of biomass burning emissions from Canada, Alaska and Siberia (*Honrath et al.*, 2004; *Val Martin et al.*, 2008a). *Val Martin et al.* (2006) reported that North American boreal wildfires contributed significantly to enhancements in CO and O_3 background mixing ratios during the summer of 2004. *Honrath et al.* (2004) also observed frequent enhancements in CO levels above the marine background levels during the summertime in 2001-2003 which they attributed to North American pollution outflow or long-range transport of biomass burning emissions. High levels of both CO and O_3 were observed during the periods of biomass burning.

CO and O_3 have been measured at PMO using instruments described in *Honrath et al.* (2004). We use hourly CO data covering 2001-2010 and O_3 data spanning 2001-2011 with most of the available data spanning May-September. Considering the diurnal variations of CO and O_3, we have applied a 24 hour filter to avoid unexpected bias – i.e. only days with full 24 hour data availability were used to calculate the daily average mixing ratios of CO and O_3. The application of this filter resulted in the inclusion of approximately 76% (87%) of the total CO (O_3) measurements in the final analysis.

2.2 Satellite data

2.2.1 AIRS/AQUA data for CO

The Atmospheric Infrared Sounder (AIRS) was launched onboard the AQUA satellite on May 4, 2002. It is a polar orbiting nadir-viewing thermal IR sounder with cloud clearing capability and retrieves CO at 4.7 microns with 70% daily global coverage; 100% between 45° and 80° longitude (*McMillan et al.*, 2005; *Yurganov et al.*, 2008). We use AIRS level 3 version 5 monthly data obtained from Giovanni, Goddard Earth Sciences Data and Information Services Center (GES DISC). Data are available at http://disc.sci.gsfc.nasa.gov/giovanni#instances (*Acker and Leptoukh*, 2007). Level 3 datasets have undergone rigorous processing and are available with no subsequent processing required. As done in prior studies, AIRS measurements with more than 0.5 degrees of freedom (*Fisher et al.*, 2010) were included in the analysis. Previous comparisons of AIRS with in-situ measurements reveal a positive bias of ~ 10% in the Northern Hemisphere (*Fisher et al.*, 2010; *Kopacz et al.*, 2010). Retrievals for the area matching the same horizontal grid as GEOS-Chem over PMO (32.5° to 27.5° W and 36° to 40° N) centered at 802 hPa (roughly 2.2 km, the same elevation as PMO) are used in this study. Since both the measurement data at PMO and GEOS-Chem use both day and night values, day and night retrievals are used for AIRS as well.

2.2.2 TES/AURA data for O_3

The Tropospheric Emission Spectrometer (TES) was launched in July, 2004 aboard the EOS Aura satellite. Data were obtained from Giovanni online data system, developed and maintained by the NASA GES DISC as mentioned above (Section 2.2.1). TES is nadir viewing in a polar orbiting sun synchronous orbit on the same track as AIRS/AQUA with a

local crossing time of 01:45 and 13:45 (*Zhang et al.*, 2010). We use available data for the period covering 2005-2010 in this study. The data for 2008 – 2009 were not available. The level three data used were pre-processed and all negative values were filtered out. Previous comparisons with in-situ measurements show that TES has a positive bias of 5.3 ppbv for O_3 at 500 hPa (*Zhang et al.*, 2010).

3 Model description

We use GEOS-Chem, a global three-dimensional model of tropospheric chemistry driven by assimilated meteorological observations from the Goddard Earth Observing System (GEOS) of the NASA Global Modeling Assimilation Office (((*Bey et al.*, 2001; *Evans and Jacob*, 2005; *Fairlie et al.*, 2007; *Martin et al.*, 2002; *Park et al.*, 2004)) to simulate the evolution of atmospheric composition in the past decade. The model has fully coupled O_3–NO_x–VOC-aerosol chemistry and has been extensively evaluated and applied to a wide range of research topics related to atmospheric chemistry and air quality (e.g., (*Duncan et al.*, 2007; *Evans and Jacob*, 2005; *Martin et al.*, 2002; *Park et al.*, 2004; *Wu et al.*, 2007)). There have been different versions of the GEOS meteorology including GEOS-3, GEOS-4 and GEOS-5 with each spanning different periods. GEOS-5 is the latest version covering the period 2004-2011. Available horizontal grid resolutions in the model range from 4° x 5° to 0.5° x 0.667° (latitude x longitude). Emission inventories in GEOS-Chem cover various sources including anthropogenic, biomass burning, biofuel and biogenic emissions. Anthropogenic emissions follow the Emissions Database for Global Atmospheric Research (EDGAR) global inventory (*Olivier and Berdowski*, 2001) and are updated with regional inventories including the U.S. EPA National Emissions Inventory (EPA/NEI05 and EPA/NEI99), the Environment Canada

National Pollutant Release (CAC) Inventory, the European Monitoring and Evaluation Program (EMEP) Inventory, the Streets Emissions Inventory in Asia (*Streets et al.,* 2006; *Streets et al.*, 2003; *Zhang et al.*, 2009) and the Big Bend Regional Aerosol and Visibility Observational (BRAVO) study emissions inventory for Mexico and some neighboring U.S. states. The biomass burning emissions follow either the Global Fire Emissions Database (GFED) v2 (1997-2008) (*van der Werf et al.,* 2006) or GFEDv3 (1997-2010) monthly inventories (*van der Werf et al.*, 2010) and biogenic VOC emissions are taken from the Model of Emissions of Gases and Aerosols from Nature (MEGAN) global inventory. Emissions from other natural sources (e.g. lightning, volcanoes) are also included. For chemistry, either the Kinetic Pre-Processor (KPP) (*Eller et al.*, 2009; *Sandu and Sander*, 2006) or the SPARSE MATRIX VECTORIZED GEAR 2 (SMVGEAR 2) (*Eller et al.*, 2009) chemistry solver can be used. The Linearized Ozone (LINOZ) mechanism (*McLinden et al.*, 2000) is used for the stratosphere-troposphere exchange of O_3.

In addition to the standard full chemistry simulations with GEOS-Chem, we also carry out special tagged simulations (tagged CO and tagged O_3 simulations) to better identify the contributions to CO and O_3 at PMO from various source regions. A brief description of the simulations used in this study and the archived data is provided in the following sections.

3.1 Full chemistry simulations used

The full chemistry simulations using the standard version of GEOS-Chem (with the SMVGEAR 2 chemical solver) with normal emissions are referred here as FCNE simulations. We used the 4° x 5° (latitude x longitude) horizontal resolution and a one year spin up for all the FCNE simulations. GEOS-4 meteorology fields were used for 2001-2004 whereas those

171 from GEOS-5 version covered the period from 2005 onwards. Regional emission inventories
172 for anthropogenic (fossil fuel & biofuel) emissions were used over Canada (CAC inventory),
173 Mexico (BRAVO), Asia (Streets), USA (NEI2005 & EPA/NEI99) and Europe (EMEP). The
174 other regions were covered by the EDGAR global anthropogenic emissions inventory.
175 Biogenic VOCs in the model include emissions of isoprene, methyl butenol and seven
176 monoterpene compounds following the MEGAN scheme (*Guenther et al.*, 2006). For biomass
177 burning emissions, the GFEDv2 monthly inventory was used (as the updated GFEDv3
178 inventory was not available with the model version (v8-03-01) used). Model simulated CO
179 and O_3 mixing ratios for the grid box covering PMO were archived with a 4 hour temporal
180 resolution. These 4 hour instantaneous mixing ratios were used to compute the daily averages
181 for both the species.
182 Table 1 summarizes the anthropogenic and biomass burning CO emissions in GEOS-Chem
183 for various regions of the Northern Hemisphere for 2001-2009. The model shows significant
184 declines in anthropogenic CO for North America and Europe but increases from Asia during
185 this time period.
186 A sensitivity run was also performed to assess the impact of North American fossil fuel
187 combustion on CO and O_3 at PMO by excluding those emissions. This run had no fossil fuel
188 emissions for the region covering the US, Canada and Mexico (15° N to 88° N (latitude) and
189 50° W to 165° W (longitude)).

190 3.2 Tagged CO simulation

191 The GEOS-Chem tagged CO simulation was used to determine the contribution to CO mixing
192 ratios at PMO from various geographical regions (e.g. Asia, North America) and sources (e.g.

biomass burning, biofuels). It is one of the several offline simulations included in GEOS-Chem and consists of source/region-specific CO tracers. The CO sources accounted for include fossil fuels, biofuels, biomass burning, anthropogenic and biogenic VOCs. A detailed description can be found in *Duncan et al.* (2007). The reaction of CO with OH is the only sink considered. We used v9-01-02 of the model with the 4° x 5° (latitude x longitude) horizontal resolution. For this simulation, emission inventories included to account for anthropogenic CO production were the global EDGAR inventory, CAC inventory over Canada, BRAVO over Mexico, EPA/NEI99 over North America, Streets over South-East Asia and the RETRO (for global anthropogenic VOCs) inventory. For biomass burning emissions, the monthly GFEDv3 emissions (available with the version used) were used. The OH concentrations used were those archived from a separate full chemistry simulation. Restart files for the tagged CO simulation were generated by an eleven month (February 2000-December 2000) spin up (with zero initial concentrations for all the tracers) for the period 2001-2004 (using GEOS-4) until steady state concentrations were reached. For the run with GEOS-5 (2005-2010), a one year spin up (January 2004-December 2004) was used. The data archived consists of the time-series of 4 hourly instantaneous values of all the CO tracers at PMO from 2001-2010. These values were used to obtain the daily average for each CO tracer.

3.3 Tagged O_3 simulation

The tagged O_3 simulation was used to attribute the O_3 mixing ratios at PMO to O_3 production from various regions. It uses chemical production/loss rates of O_3 archived from the FCNE simulation. We used version 09-01-02 of GEOS-Chem (horizontal resolution 4° x 5° (latitude x longitude)) for this simulation and the same version was also used to archive the O_3

production/loss rates from 2000-2011. Restart files were generated in the same manner as for the tagged CO simulation. The time-series of 4 hourly instantaneous values of all the tracers was archived from 2001-2011 for the location and altitude corresponding to PMO. The daily averages for all tracers were computed using these 4-hourly instantaneous values.

4 GEOS-Chem model evaluation

GEOS-Chem output for CO and O_3 mixing ratios was compared with the in situ measurement data for the two species at PMO as well as satellite retrievals from AIRS/AQUA (for CO) and TES/AURA (for O_3). Figure 2 shows the time series of 24-hour average O_3 and CO mixing ratios at PMO from September 2000 – August 2010 along with the 24-hour averages computed from GEOS-Chem time series output for this period. For CO, GEOS-Chem was found to underestimate the observations with the magnitude during summer being 24.7 +/- 5.2 ppbv (1-□). The significant underestimate of CO by GEOS-Chem possibly reflects some low biases in the CO emission inventories used in the model. The model underestimates of CO have also been reported by previous studies (*Bey et al.*, 2001; *Duncan and Logan*, 2008; *Duncan et al.*, 2007; *Val Martin et al.*, 2008b). For O_3, the GEOS-Chem performance was much better. The model was 6.7 +/- 2.6 ppbv higher and showed the least agreement in winter and best agreement in summer and fall.

The seasonal variation of CO and O_3 at PMO was further examined in Figure 3 with box plots for GEOS-Chem model simulations (24 hour averages) compared with ground-based in situ measurements and satellite data. The data used in Figure 3 covers the period of September 2004 to August 2005 as this period has the best data availability for the measurements. Both

Figures 2 and 3 show that the seasonal variations associated with CO and O_3 are well captured by GEOS-Chem. Both species show maxima in the spring-time and minima in the summer-time with consistency between the model results and measurement data. Similar seasonal variations have also been reported for these species at other remote sites such as Mace Head (*Derwent et al.*, 1998) and mountaintop stations such as Mt. Cimone (*Bonasoni et al.*, 2000) and for CO in a previous study at the PMO (*Val Martin et al.*, 2008b). The AIRS data further confirms the model underestimate of CO which is particularly large during late spring – early summer. We also compared model results with observational data on the inter-annual variability of O_3 at PMO (Figure 4). The period of May-August was chosen for best data coverage and average O_3 mixing ratio for this period was calculated for each year. Some years without sufficient observational data coverage were excluded from the comparison. We find that besides the period of 2004-2006, the inter-annual variability of O_3 at PMO reflected from the GEOS-Chem model results generally agrees well with the observational data (Figure 4).

5 General Long term trends of CO and O_3 at PMO

5.1 Trend analysis methodology

Two-sided parametric hypothesis testing (null hypothesis of no trend and alternate hypothesis of non-zero trend) was used to analyze the trends in CO and O_3 mixing ratios at PMO for 2001-2011. We employed a multiple regression model that is similar to the additive model of a time-series and contains sinusoidal functions to represent the characteristic seasonal variations of both CO and O_3. The sinusoidal functions use a time period of one year to reflect the seasonal variations of CO and O_3. A linear term in time was used to represent the long

term trend in CO or O_3. Following *Helsel and Hirsch* (2002), we express the model for daily average values of CO or O_3 as:

$$\mathbf{C_t = a_0 + a_1 t + a_2 sin\left(\frac{2\pi t}{365}\right) + a_3 cos\left(\frac{2\pi t}{365}\right) + \varepsilon_t} \quad (1)$$

Where:

$\mathbf{C_t}$: Mixing ratio of the species at a time t (in days of year) (time being measured from a reference year (01/01/1900 in this case))

$\mathbf{a_0, a_1, a_2, a_3}$: regression coefficients

$\boldsymbol{\varepsilon_t}$: residual from the model

For all datasets consisting of daily averages, a five day centered simple moving average scheme was applied to the data before fitting the regression model. Coefficients in the regression equation were determined by the least squares method and the statistical significance of the t-statistic corresponding to the slope term was examined by comparing the probability of observing a t-statistic of same or greater magnitude with the null hypothesis being true (p-value) with the significance level α (0.05 used for this study).

5.2 Trends obtained from PMO data and GEOS-Chem results

The regression model in Eq. (1) was applied to the time-series of CO and O_3 (for both the in-situ measurements and GEOS-Chem FCNE simulation output) at PMO. Table 2 lists the trends for both the measurement data and GEOS-Chem output along with the associated p-values. Figure 5 shows the regression fits for the CO and O_3 measurements and Figure 6 contains the fits for the modeled (GEOS-Chem FCNE simulation) CO and O_3. The observations show statistically significant decreasing trends for both the species over the study period with CO showing a decrease of -0.31 +/- 0.30 (2-σ) ppbv yr^{-1} (p-value = 0.04) and O_3

278 decreasing by -0.21 +/- 0.11 (2-σ) ppbv yr^{-1} (p-value < 0.001). GEOS-Chem also shows
279 statistically significant decreasing trends for both CO (-0.34 +/- 0.08 (2-σ) ppbv yr^{-1}, p-value
280 < 0.001) and O_3 (-0.53 +/- 0.04 (2-σ) ppbv yr^{-1}, p-value < 0.001).
281 These decreasing trends are in agreement with those obtained from observation data at other
282 stations in the North Atlantic such as Tudor Hill, Bermuda (TH) and Mace Head, Ireland (MH)
283 (data available at http://ds.data.jma.go.jp/gmd/wdcgg/cgi-bin/wdcgg/catalogue.cgi). For TH,
284 the harmonic regression analysis of O_3 mixing ratios from 2003-2011 yields a statistically
285 significant decreasing trend (p-value < 0.001) of 1.1 +/- 0.11 (2-σ) ppbv yr^{-1}, whereas CO at
286 MH (2001-2011) shows a statistically significant decreasing trend (-1.4 +/- 0.20 (2-σ) ppbv
287 yr^{-1}, p-value < 0.001) as well. However, measurements at Izana, Tenerife (IT) (data available
288 at http://ds.data.jma.go.jp/gmd/wdcgg/cgi-bin/wdcgg/catalogue.cgi) show an increasing trend
289 of 0.10 +/- 0.07 (2-σ) ppbv yr^{-1} for O_3 over the study period. This opposite trend at IT could
290 indicate the fact that it is further south and less affected by the continental outflow from North
291 America. Previous studies such as *Lelieveld et al.* (2004) and *Derwent et al.* (2007) have
292 reported upward trends in O_3 over the North Atlantic for the periods 1977-2002 and 1987-
293 2007 respectively. The discrepancy appears largely due to the different time frame used in
294 these studies. This factor is exemplified by the different trends observed for O_3 at TH
295 (increasing trend of 0.70 +/- 0.10 (2-σ) ppbv yr^{-1}, p-value < 0.001) for the earlier decade of
296 1988-1998 as compared to the decreasing trend for 2003-2011.
297 One of the major factors that could lead to a decrease in CO and O_3 mixing ratios over the
298 North Atlantic is the decline in anthropogenic emissions from North America (of which 80%
299 emissions are from the U.S.) in the past decade. The trends for U.S. anthropogenic emissions
300 of CO and NO_x are shown in Figure 1. In order to investigate this hypothesis we first carried

out sensitivity runs by turning off North American fossil fuel emissions in the model (Section 3.1) to derive the contribution of North American anthropogenic emissions to CO and O_3 at PMO. Our results show that the anthropogenic emissions from North America enhance the annual means of CO and O_3 at PMO by 8.6 and 4.0 ppbv yr^{-1} respectively (Table 3). Also, Figure 1 shows that the U.S. CO emissions have declined by about 1/3, from around 105 Tg in 2000 to 70 Tg in 2011. Assuming a linear correspondence between the U.S. emissions and their contribution to CO mixing ratios at PMO, this would amount to a decrease of approximately 2.9 ppbv in the CO at the station (over the past decade). This change is similar to that obtained from the harmonic regression analysis of CO measurements at PMO, suggesting that the observed possible decline in the CO at the station correlates particularly well with the U.S. emission declines. For CO, the largest contribution from North American emissions was found in the winter and spring, which reflects stronger atmospheric transport and longer chemical lifetimes of CO (due to low levels of OH) during those seasons, as previously noted by (*Val Martin et al.*, 2008b). In contrast, for O_3, the least North American contribution was found during winter reflecting the NO_x-saturated regime where O_3 production is more sensitive to the photochemically generated hydrogen oxide radicals (HO_x) (*Jacob et al.*, 1995; *Kleinman et al.*, 1995).

In order to better understand and quantify the effects associated with the decreases in North American emissions, we also carried out tagged CO and O_3 simulations with the GEOS-Chem model. Results of the trend analysis for the tagged CO simulation are summarized in Table 4. The contribution of CO produced from anthropogenic fossil fuel emissions in the U.S. to CO at PMO shows a statistically significant (p-value < 0.001) decrease over the study period. The contribution of biomass burning emissions in Europe also shows a statistically significant (p-

value < 0.001) decrease. On the other hand, contribution of fossil fuel emissions in Asia shows a statistically significant (p-value < 0.001) increase. These results indicate that reductions in CO from North America and Europe could be the primary reasons for the possible decrease in CO at PMO, which outweigh the effects of increasing CO from Asia in the past decade.

Table 5 summarizes the results of the statistical analysis for the tagged O_3 simulation. Statistically significant (p-value < 0.001) decreasing trends are obtained for the contributions to O_3 at PMO from O_3 production in the boundary layer over various regions including North America, Europe and Asia. The contribution of O_3 production in the middle troposphere (MT) (Boundary Layer top – 350 hPa) also shows a decreasing trend (p-value < 0.001) over the study period. On the other hand, an increasing trend (p-value < 0.001) was identified for the contribution from O_3 produced in the upper troposphere (UT) (350 hPa – tropopause).

The decreasing trends for contributions to O_3 at PMO from North America and Europe are consistent with the declines in anthropogenic O_3 precursor emissions in these regions. On the other hand, the decrease in the contribution of O_3 produced in Asia (where anthropogenic precursor emissions have been increasing) may reflect the impacts from climate change in the past decade. Except for regions with strong emissions of O_3 precursors, climate change generally decreases surface O_3 due to enhanced O_3 destruction associated with higher water vapor concentration in the atmosphere (e.g., (*Johnson et al.*, 1999; *Wu et al.*, 2008)). With reduced chemical lifetime of O_3, this effect is particularly important for remote regions and the long range transport of atmospheric O_3. Analysis of the atmospheric water vapor concentrations in the past decade shows significant increases (up to 20%) over the North Atlantic for the study period which contributes to a shorter O_3 lifetime during transport. The increase in the contribution of O_3 produced in the UT could be due to an increase in the NO_x

production from lightning. Harmonic regression analysis of global lightning flashes archived from GEOS-Chem for 2001-2011 shows statistically significant increase over this period which points to an increase in the NO_x produced. The upper troposphere O_3 is highly sensitive to NO_x emissions from lightning, with the O_3 production efficiency (referenced to NO_x emissions) about six times higher than that for NO_x emissions in surface air (*Wu et al.*, 2008). The statistically significant decreasing trend for the contribution of O_3 production in the North Atlantic largely reflects the decline in the anthropogenic emissions from North America. When comparing the contributions from various regions (North America, Europe and Asia) in Table 5, we can see that the reductions in anthropogenic emissions of O_3 precursors is the most important factor contributing to the possible decrease in O_3 mixing ratios observed at PMO.

6 Conclusions and Summary

This study analyzes in-situ measurements of CO and O_3 at the Pico mountaintop observatory and output from GEOS-Chem model simulations to determine the trends in CO and O_3 over the North Atlantic region for the past decade. The GEOS-Chem model performance is also evaluated by comparing simulation results against measurements at PMO and satellite output. The model reproduces the seasonal variations of CO and O_3 at PMO reasonably well although it significantly underestimates CO at this remote site.

Sensitivity studies show that North American fossil fuel emissions account for 8.6 and 4.0 ppbv CO and O_3, respectively, of the total mixing ratios observed at PMO. This contribution to the CO mixing ratios is greatest during winter and spring, reflecting the longer CO lifetimes

368 and stronger transport during those seasons. In contrast, the contribution to the O_3 is found to
369 be smallest during winter reflecting the low O_3 production and low sensitivity to NO_x
370 emissions during wintertime.

371 Harmonic regression analysis of the observed CO and O_3 mixing ratios at PMO for 2001-2011
372 shows statistically significant decreases for both species. The best estimates of the possible
373 trends for the CO and O_3 measurements are -0.31 +/- 0.30 (2-σ) ppbv yr^{-1} and -0.21 +/- 0.11
374 (2-σ) ppbv yr^{-1} respectively. GEOS-Chem model simulations for the past decade also yield
375 decreasing trends for CO and O_3 at PMO. We conducted tagged simulations for CO and O_3
376 respectively with GEOS-Chem to attribute these decreases. Contribution to CO at PMO from
377 fossil fuel emissions in the United States shows a statistically significant decreasing trend (-
378 0.27 +/- 0.05 (2-σ) ppbv yr^{-1}) while the contribution from fossil fuel emissions in Asia shows
379 a statistically significant increasing trend (+0.35 +/- 0.03 (2-σ) ppbv yr^{-1}). Also, biomass
380 burning emissions in Europe show statistically significant decreasing contribution (-0.3 +/-
381 0.03 (2-σ) ppbv yr^{-1}). These results indicate that even though the increasing CO emissions
382 from Asia in the past decade have led to increasing enhancement in CO over the North
383 Atlantic, the decreases in CO from North America and Europe more than compensate these
384 increases and result in an overall possible decrease in CO mixing ratios at PMO. The changes
385 in O_3 at PMO are attributed to O_3 production in various regions (e.g., North America, North
386 Atlantic, Europe and Asia) through tagged O_3 simulations with the GEOS-Chem model.
387 Contributions from O_3 produced in the lower and middle troposphere also show statistically
388 significant decreasing trends. The decreases in the contribution of O_3 from North America and
389 Europe as well as the North Atlantic are consistent with the decreases in anthropogenic
390 emissions of O_3 precursors in North America and Europe in the past decade. While the

391 anthropogenic emissions in Asia have increased in the past decade, the decreasing trend for
392 contribution to PMO O_3 from Asia possibly reflects the impacts of climate change which is
393 expected to enhance the destruction and therefore reduce the long-range transport of O_3.
394 Overall, the emission reduction of O_3 precursors in North America in the past decade is the
395 most important factor contributing to the possible decreasing trends of CO and O_3 at PMO.

396

397 **Acknowledgement**

398 This research and the operation of the Pico Mountain Observatory have been supported by
399 several agencies, including the NSF Atmospheric Chemistry program, the NOAA Office of
400 Global Programs, and the Regional Government of the Azores, and through funding from the
401 UK National Environment Research Council for the BORTAS project. This publication was
402 made possible by USEPA STAR grant (83518901). Its contents are solely the responsibility
403 of the grantee and do not necessarily represent the official views of the USEPA. Further,
404 USEPA does not endorse the purchase of any commercial products or services mentioned in
405 the publication.

406

407

408

409

410

References

Acker, J. G., and Leptoukh, G. (2007), Online analysis enhances use of NASA Earth science data, *Eos, Transactions American Geophysical Union*, *88*(2), 14-17.

Bey, I., Jacob, D. J., Yantosca, R. M., Logan, J. A., Field, B. D., Fiore, A. M., Li, Q., Liu, H. Y., Mickley, L. J., and Schultz, M. G. (2001), Global modeling of tropospheric chemistry with assimilated meteorology: Model description and evaluation, *Journal of geophysical research*, *106*(D19), 23 073-023 096.

Bonasoni, P., Stohl, A., Cristofanelli, P., Calzolari, F., Colombo, T., and Evangelisti, F. (2000), Background ozone variations at Mt. Cimone station, *Atmos Environ*, *34*(29), 5183-5189.

Brunke, E., Meyer, C., Lathrop, J., Johnson, B., Shadwick, D., Cuevas, E., Schmidlin, F., Tarasick, D., Claude, H., and Kerr, J. (1998), Trends of ozone in the troposphere, *Geophys Res Lett*, *25*(2), 139-142.

Derwent, R. G., Simmonds, P. G., Seuring, S., and Dimmer, C. (1998), Observation and interpretation of seasonal cycles in the surface concentrations of ozone and carbon monoxide at Mace Head, Ireland, from 1990 to 1994, *Atmos Environ*, *32*(2), 145-157, doi:110.1016/S1352-2310(1097)00338-00335.

Derwent, R. G., Simmonds, P. G., Manning, A. J., and Spain, T. G. (2007), Trends over a 20-year period from 1987 to 2007 in surface ozone at the atmospheric research station, Mace Head, Ireland, *Atmos Environ*, *41*(39), 9091-9098.

Duncan, B. N., and Logan, J. A. (2008), Model analysis of the factors regulating the trends and variability of carbon monoxide between 1988 and 1997, *Atmos Chem Phys*, *8*(24), 7389-7403, doi:7310.5194/acp-7388-7389-2008.

Duncan, B. N., Logan, J. A., Bey, I., Megretskaia, I. A., Yantosca, R. M., Novelli, P. C., Jones, N. B., and Rinsland, C. P. (2007), Global budget of CO, 1988–1997: Source estimates and validation with a global model, *Journal of geophysical research*, *112*(D22), D22301, DOI: 22310.21029/22007JD008459.

Eller, P., Singh, K., Sandu, A., Bowman, K., Henze, D. K., and Lee, M. (2009), Implementation and evaluation of an array of chemical solvers in the Global Chemical Transport Model GEOS-Chem, *Geoscientific Model Development*, *2*, 89-96, doi:10.5194/gmd-5192-5189-2009.

Evans, M. J., and Jacob, D. J. (2005), Impact of new laboratory studies of N2O5 hydrolysis on global model budgets of tropospheric nitrogen oxides, ozone, and OH, *Geophys Res Lett*, *32*(9), L09813, doi:09810.01029/02005GL022469.

Fairlie, T. D., Jacob, D. J., and Park, R. J. (2007), The impact of transpacific transport of mineral dust in the United States, *Atmos Environ*, *41*(6), 1251-1266.

Fisher, J. A., et al. (2010), Source attribution and interannual variability of Arctic pollution in spring constrained by aircraft (ARCTAS, ARCPAC) and satellite (AIRS) observations of carbon monoxide, *Atmos Chem Phys*, *10*(3), 977-996, doi:910.5194/acp-5110-5977-2010.

Fusco, A. C., and Logan, J. A. (2003), Analysis of 1970–1995 trends in tropospheric ozone at Northern Hemisphere midlatitudes with the GEOS-CHEM model, *Journal of Geophysical Research: Atmospheres (1984–2012)*, *108*(D15), doi:10.1029/2002JD002742.

Guenther, A., Karl, T., Harley, P., Wiedinmyer, C., Palmer, P. I., and Geron, C. (2006), Estimates of global terrestrial isoprene emissions using MEGAN (Model of Emissions of Gases and Aerosols from Nature), *Atmos Chem Phys*, *6*(11), 3181-3210, doi:3110.5194/acp-3186-3181-2006.

Guicherit, R., and Roemer, M. (2000), Tropospheric ozone trends, *Chemosphere-Global Change Science*, *2*(2), 167-183.
Helsel, D. R., and Hirsch, R. M. (2002), *Statistical methods in water resources*, US Geological survey Reston, Va.
Holloway, T., Hiram Levy, I., and Kasibhatla, P. (2000), Global distribution of carbon monoxide, *Journal of Geophysical Research*, *105*(D10), 12123-12112,12147.
Honrath, R. E., Owen, R. C., Val Martin, M., Reid, J. S., Lapina, K., Fialho, P., Dziobak, M. P., Kleissl, J., and Westphal, D. L. (2004), Regional and hemispheric impacts of anthropogenic and biomass burning emissions on summertime CO and O3 in the North Atlantic lower free troposphere, *J Geophys Res-Atmos*, *109*(D24), doi:10.1029/2004JD005147.
Hudman, R. C., Murray, L. T., Jacob, D. J., Turquety, S., Wu, S., Millet, D. B., Avery, M., Goldstein, A. H., and Holloway, J. (2009), North American influence on tropospheric ozone and the effects of recent emission reductions: Constraints from ICARTT observations, *Journal of Geophysical Research: Atmospheres (1984–2012)*, *114*(D7), doi:10.1029/2008JD010126.
Jacob, D. J., Horowitz, L. W., Munger, J. W., Heikes, B. G., Dickerson, R. R., Artz, R. S., and Keene, W. C. (1995), Seasonal transition from NOx-to hydrocarbon-limited conditions for ozone production over the eastern United States in September, *Journal of Geophysical Research: Atmospheres (1984–2012)*, *100*(D5), 9315-9324.
Jaffe, D., Price, H., Parrish, D., Goldstein, A., and Harris, J. (2003), Increasing background ozone during spring on the west coast of North America, *Geophys Res Lett*, *30*(12), 1613, doi:1610.1029/2003GL017024.
Johnson, C. E., Collins, W. J., Stevenson, D. S., and Derwent, R. G. (1999), Relative roles of climate and emissions changes on future tropospheric oxidant concentrations, *Journal of Geophysical Research: Atmospheres (1984–2012)*, *104*(D15), 18631-18645.
Khalil, M. A. K., and Rasmussen, R. A. (1994), Global decrease in atmospheric carbon monoxide *Nature*, *370*(25), 639-641.
Kleinman, L., Lee, Y. N., Springston, S. R., Lee, J. H., Nunnermacker, L., Weinstein-Lloyd, J., Zhou, X., and Newman, L. (1995), Peroxy radical concentration and ozone formation rate at a rural site in the southeastern United States, *Journal of geophysical research*, *100*(D4), 7263-7273.
Kleissl, J., Honrath, R. E., Dziobak, M. P., Tanner, D., Martin, M. V., Owen, R. C., and Helmig, D. (2007), Occurrence of upslope flows at the Pico mountaintop observatory: A case study of orographic flows on a small, volcanic island, *JOURNAL OF GEOPHYSICAL RESEARCH-ALL SERIES-*, *112*(D10), 10, DOI: 10.1029/2006JD007565.
Kopacz, M., et al. (2010), Global estimates of CO sources with high resolution by adjoint inversion of multiple satellite datasets (MOPITT, AIRS, SCIAMACHY, TES), *Atmos Chem Phys*, *10*(3), 855-876, doi:810.5194/acp-5110-5855-2010.
Law, K. (2010), More ozone over North America, *Nature*, *463*, 307-308.
Lee, S. H., Akimoto, H., Nakane, H., Kurnosenko, S., and Kinjo, Y. (1998), Lower tropospheric ozone trend observed in 1989-1997 at Okinawa, Japan, *Geophys Res Lett*, *25*(10), 1637-1640.
Lelieveld, J., Van Aardenne, J., Fischer, H., De Reus, M., Williams, J., and Winkler, P. (2004), Increasing ozone over the Atlantic Ocean, *Science*, *304*(5676), 1483-1487.
Li, Q., et al. (2002), Transatlantic transport of pollution and its effects on surface ozone in Europe and North America, *J. Geophys. Res*, *107*(10.1029), DOI: 10.1029/2001JD001422.
Martin, R. V., et al. (2002), An improved retrieval of tropospheric nitrogen dioxide from GOME, *Journal of Geophysical Research: Atmospheres (1984–2012)*, *107*(D20), 4437-4456, DOI: 4410.1029/2001JD001027.

McLinden, C. A., Olsen, S. C., Hannegan, B., Wild, O., Prather, M. J., and Sundet, J. (2000), Stratospheric ozone in 3-D models: A simple chemistry and the cross-tropopause flux, *J Geophys Res-Atmos*, *105*(D11), 14653-14665, DOI: 14610.11029/12000JD900124.

McMillan, W. W., Barnet, C., Strow, L., Chahine, M. T., McCourt, M. L., Warner, J. X., Novelli, P. C., Korontzi, S., Maddy, E. S., and Datta, S. (2005), Daily global maps of carbon monoxide from NASA's Atmospheric Infrared Sounder, *Geophys Res Lett*, *32*(11), L11801, doi:11810.11029/12004GL021821.

Olivier, J. G. J., and Berdowski, J. J. M. (2001), Global emission sources and sinks, 33-77.

Oltmans, S. J., et al. (2006), Long-term changes in tropospheric ozone, *Atmos Environ*, *40*(17), 3156-3173.

Park, R. J., Jacob, D. J., Field, B. D., Yantosca, R. M., and Chin, M. (2004), Natural and transboundary pollution influences on sulfate-nitrate-ammonium aerosols in the United States: Implications for policy, *Journal of Geophysical Research: Atmospheres (1984–2012)*, *109*(D15), doi:10.1029/2003JD004473.

Sandu, A., and Sander, R. (2006), Technical note: Simulating chemical systems in Fortran90 and Matlab with the Kinetic PreProcessor KPP-2.1, *Atmos Chem Phys*, *6*(1), 187-195.

Seinfeld, J. H., and Pandis, S. N. (2006), Atmospheric Chemistry and Physics: From Air Pollution to Climate Change, *Atmospheric Chemistry and Physics, John Wiley & Sons, New York*, *1326*.

Streets, D. G., Zhang, Q., Wang, L., He, K., Hao, J., Wu, Y., Tang, Y., and Carmichael, G. R. (2006), Revisiting China's CO emissions after the Transport and Chemical Evolution over the Pacific (TRACE-P) mission: Synthesis of inventories, atmospheric modeling, and observations, *Journal of geophysical research*, *111*(D14), D14306, DOI: 14310.11029/12006JD007118.

Streets, D. G., et al. (2003), An inventory of gaseous and primary aerosol emissions in Asia in the year 2000, *Journal of geophysical research*, *108*(D21), 8809, DOI: 8810.1029/2002JD003093.

Val Martin, M., Honrath, R. E., Owen, R. C., and Lapina, K. (2008a), Large-scale impacts of anthropogenic pollution and boreal wildfires on the nitrogen oxides over the central North Atlantic region, *Journal of geophysical research*, *113*(D17), D17308, DOI: 17310.11029/12007JD009689.

Val Martin, M., Honrath, R. E., Owen, R. C., and Li, Q. B. (2008b), Seasonal variation of nitrogen oxides in the central North Atlantic lower free troposphere, *Journal of Geophysical Research: Atmospheres (1984–2012)*, *113*(D17), doi:10.1029/2007JD009688.

Val Martin, M., Honrath, R. E., Owen, R. C., Pfister, G., Fialho, P., and Barata, F. (2006), Significant enhancements of nitrogen oxides, black carbon, and ozone in the North Atlantic lower free troposphere resulting from North American boreal wildfires, *J. Geophys. Res*, *111*, D23S60.

van der Werf, G. R., Randerson, J. T., Giglio, L., Collatz, G. J., Kasibhatla, P. S., and Arellano Jr, A. F. (2006), Interannual variability of global biomass burning emissions from 1997 to 2004, *Atmospheric Chemistry and Physics Discussions*, *6*(2), 3175-3226.

van der Werf, G. R., Randerson, J. T., Giglio, L., Collatz, G. J., Mu, M., Kasibhatla, P. S., Morton, D. C., DeFries, R. S., Jin, Y., and van Leeuwen, T. T. (2010), Global fire emissions and the contribution of deforestation, savanna, forest, agricultural, and peat fires (1997–2009), *Atmos. Chem. Phys*, *10*(23), 11,707-711,735, doi:710.5194/acp-5110-11707-12010.

Vingarzan, R. (2004), A review of surface ozone background levels and trends, *Atmos Environ*, *38*(21), 3431-3442.

Wang, H., Jacob, D. J., Le Sager, P., Streets, D. G., Park, R. J., Gilliland, A. B., and Van Donkelaar, A. (2009), Surface ozone background in the United States: Canadian and Mexican pollution influences, *Atmos Environ*, *43*(6), 1310-1319.

Wang, Y., Jacob, D. J., and Logan, J. A. (1998), Global simulation of tropospheric O3-NOx-hydrocarbon chemistry. 1. Model formulation, *J. Geophys. Res*, *156*, 148-227.

Wu, S., Mickley, L. J., Jacob, D. J., Logan, J. A., Yantosca, R. M., and Rind, D. (2007), Why are there large differences between models in global budgets of tropospheric ozone?, *Journal of geophysical research*, *112*(D5), D05302, doi:05310.01029/02006JD007801.

Wu, S., Mickley, L. J., Leibensperger, E. M., Jacob, D. J., Rind, D., and Streets, D. G. (2008), Effects of 2000–2050 global change on ozone air quality in the United States, *Journal of geophysical research*, *113*(D6), D06302, DOI: 06310.01029/02007JD009639.

Yurganov, L. N., McMillan, W. W., Dzhola, A. V., Grechko, E. I., Jones, N. B., and van der Werf, G. R. (2008), Global AIRS and MOPITT CO measurements: Validation, comparison, and links to biomass burning variations and carbon cycle, *Journal of Geophysical Research: Atmospheres (1984–2012)*, *113*(D9), doi:10.1029/2007JD009229.

Zhang, L., Jacob, D. J., Liu, X., Logan, J. A., Chance, K., Eldering, A., and Bojkov, B. R. (2010), Intercomparison methods for satellite measurements of atmospheric composition: application to tropospheric ozone from TES and OMI, *Atmos Chem Phys*, *10*(10), 4725-4739, doi:4710.5194/acp-4710-4725-2010.

Zhang, Q., Streets, D. G., Carmichael, G. R., He, K. B., Huo, H., Kannari, A., Klimont, Z., Park, I. S., Reddy, S., and Fu, J. S. (2009), Asian emissions in 2006 for the NASA INTEX-B mission, *Atmos. Chem. Phys*, *9*(14), 5131-5153, doi:5110.5194/acp-5139-5131-2009.

575 Table 1. Anthropogenic and biomass burning CO emissions used in GEOS-Chem (values

576 are in Tg CO yr^{-1})

	Anthropogenic				Biomass Burning	
Year	Northern Hemisphere	North America	Europe	Asia	Northern Hemisphere	North America
2001	436.5	97.3	45.1	245.9	202.6	8.7
2002	447.9	99.9	42.8	256.0	230.9	21.3
2003	460.3	95.5	41.6	272.9	246.5	33.9
2004	461.1	90.6	41.6	278.1	201.0	23.2
2005	460.1	86.3	40.0	281.8	216.0	20.7
2006	460.7	83.0	38.2	286.2	180.9	15.5
2007	455.9	83.0	35.4	286.2	219.6	15.3
2008	457.2	83.2	35.6	287.0	180.9	13.8
2009	455.9	83.0	35.4	286.2	180.0	13.8

577

578

579

580

581

582

583

584

585

586

587

588

589

590

591

592

593

Table 2: CO and O_3 trends obtained for PMO observations and GEOS-Chem output

Species	Trend (ppbv yr^{-1})*		P-value	
	Observations	GEOS-Chem	Observations	GEOS-Chem
CO	-0.31 +/- 0.30	-0.34 +/- 0.08	0.04	< 0.001
O_3	-0.21 +/- 0.11	-0.53 +/- 0.04	< 0.001	< 0.001

***** Uncertainties are in the 2-σ (95%) interval

Table 3: GEOS-Chem North American fossil fuel emissions contribution to mixing ratios of CO and O_3 at PMO (means for every season from fall 2000 to summer 2010)

Season	CO (ppbv)	O_3 (ppbv)
Fall	5.7	4.4
Winter	12.7	2.3
Spring	11.0	4.5
Summer	4.9	4.9
Annual	8.6	4.0

Table 4: Trends in contributions to CO at PMO from various regions and sources[1]

CO source[2]	Trend (ppbv yr^{-1})*	P-value
CO (ff USA)	-0.27 +/- 0.05	< 0.001
CO (ff Europe)	-0.004 +/- 0.03	0.39
CO (ff Asia)	+0.35 +/- 0.03	< 0.001
CO (bb North America)	-0.03 +/- 0.02	0.004
CO (bb Europe)	-0.30 +/- 0.03	< 0.001
CO (bb Asia)	+0.05 +/- 0.01	< 0.001

1. Results based on GEOS-Chem tagged CO simulation results
2. ff=emissions from fossil fuel combustion; bb=emissions from biomass burning

***** Uncertainties are in the 2-σ (95%) interval

Table 5: Trends in contributions to O_3 at PMO from various regions and sources[1]

O_3 source[2]	Trend (ppbv yr^{-1})*	P-value
O_3 (produced over the USA)	-0.18 +/- 0.03	< 0.001
O_3 (produced in the NA BL)	-0.57 +/- 0.02	< 0.001
O_3 (produced in the Asian BL)	-0.12 +/- 0.004	< 0.001
O_3 (produced in the European BL)	-0.09 +/- 0.003	< 0.001
O_3 (produced in the NAtl BL)	-0.51 +/- 0.02	< 0.001
O_3 (produced in the UT)	+3.13 +/- 0.07	< 0.001
O_3 (produced in the MT)	-2.19 +/- 0.05	< 0.001

1. Results based on GEOS-Chem tagged O_3 simulation results
2. NA: North America, BL: Boundary Layer, NAtl: North Atlantic, UT: Upper Troposphere, MT: Middle Troposphere

***** Uncertainties are in the 2-σ (95%) interval

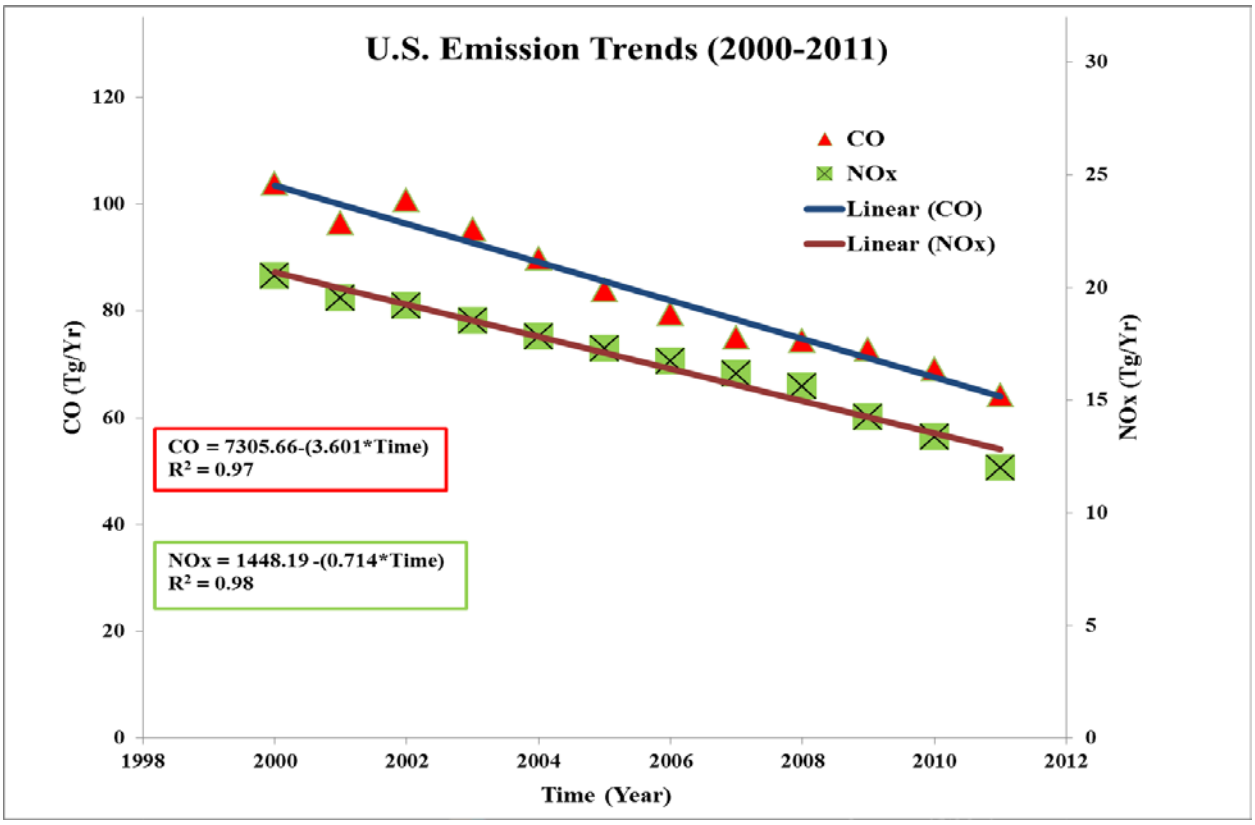

Figure 1: U.S. anthropogenic emissions (in Tg yr^{-1}) for CO and NO_x from 2000 to 2011. (Data available at: http://www.epa.gov/ttnchie1/trends/)

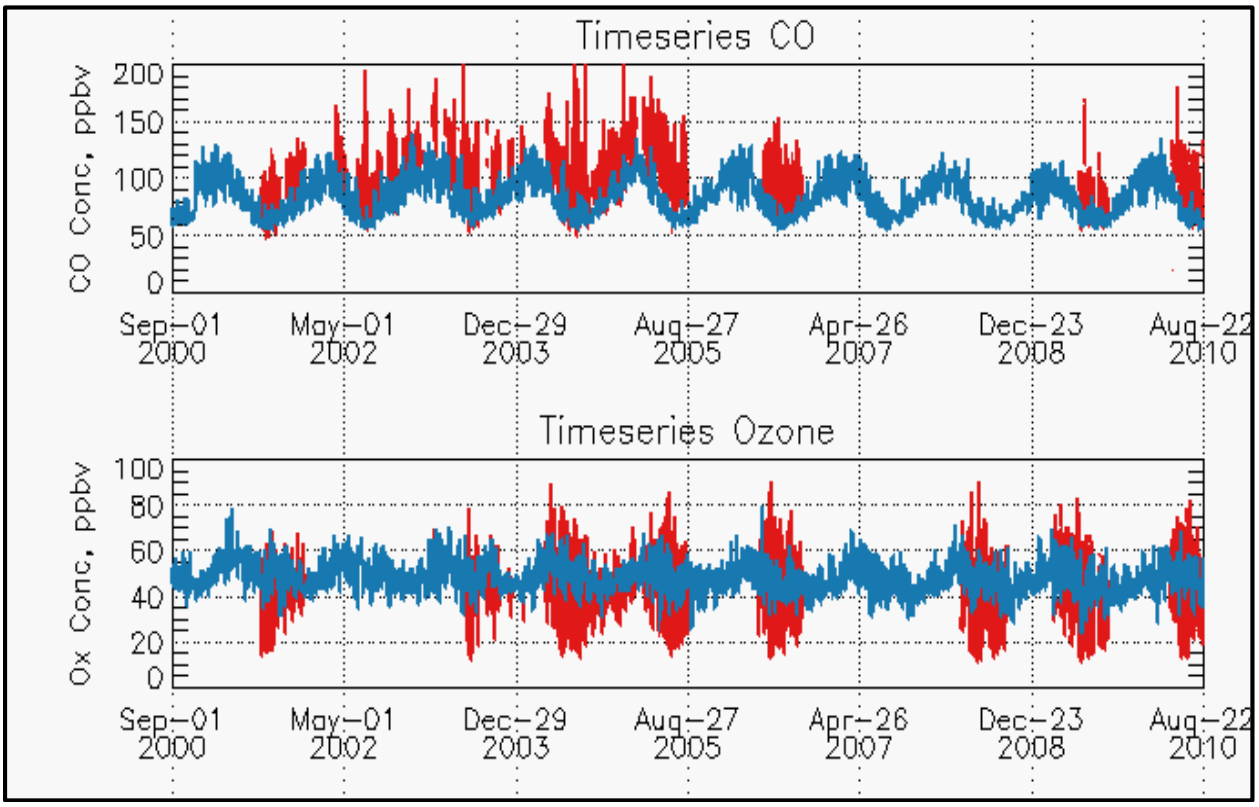

Figure 2: Time-series of CO (top) and O_3 (bottom) from September 2000 – August 2010. The observations (hourly mixing ratios) are shown in red and GEOS-Chem output (4 hourly instantaneous mixing ratios) are shown in blue.

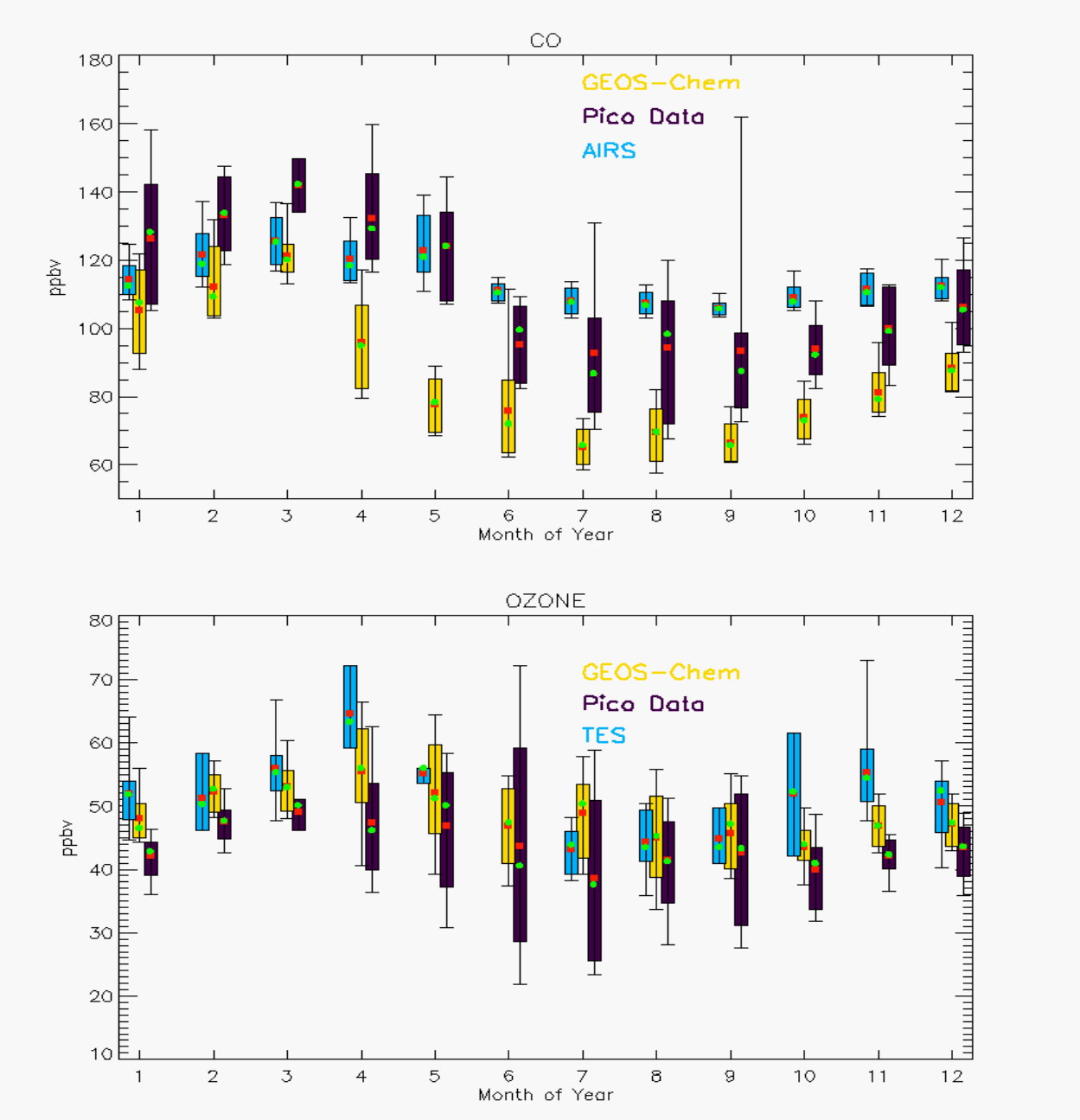

Figure 3. Seasonal variation of CO (top) and O_3 (bottom) at PMO (September 2004-August 2005) . GEOS-Chem model simulations (yellow), in-situ measurements (dark brown) and satellite observations (AIRS for CO and TES for O_3) (light blue). The thick (thin) bars represent the 67% (90%) confidence intervals. The mean and median are represented with red and green dots respectively.The statistics are based on daily (24 hour) averages.

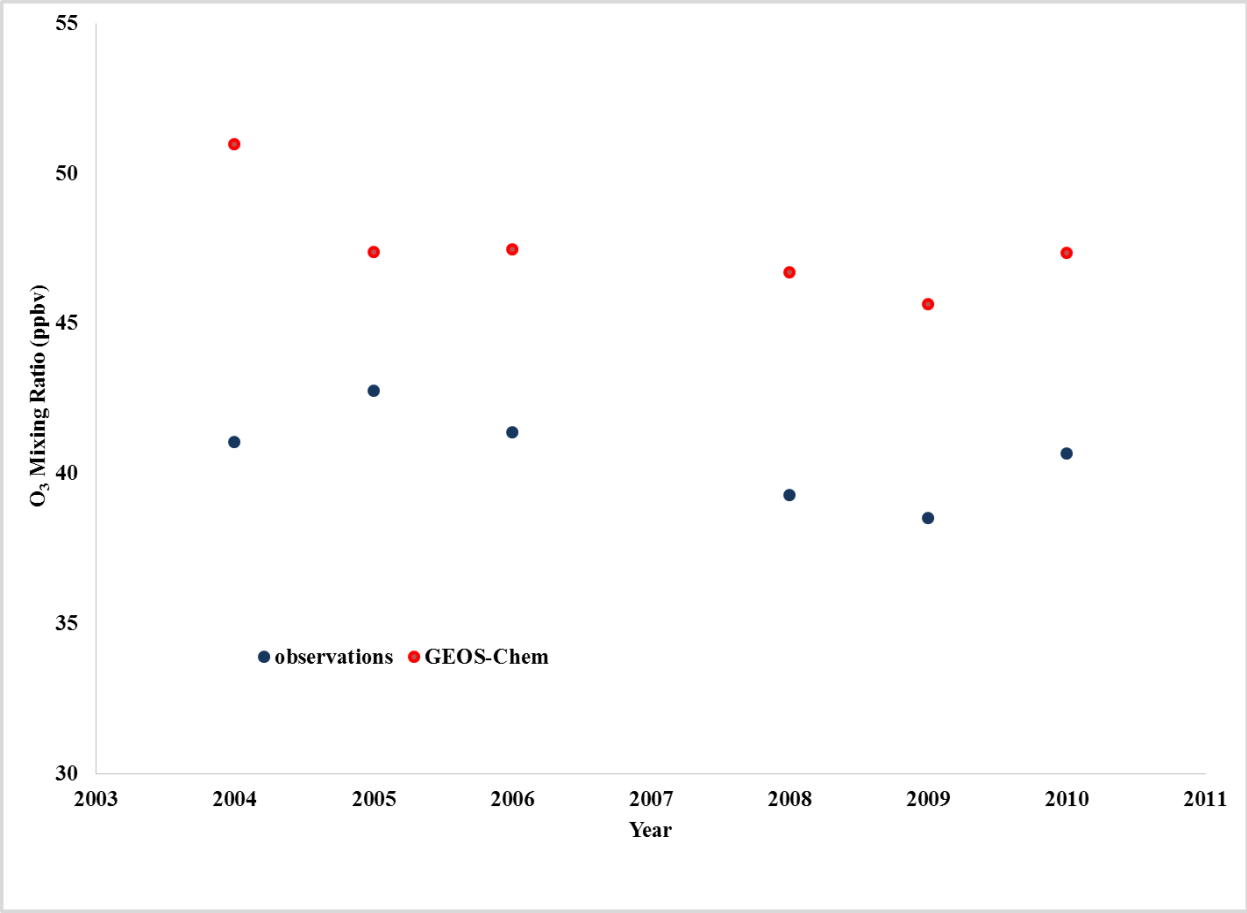

Figure 4: May - August averages for O_3. The observations are shown in blue and GEOS-Chem output in red.

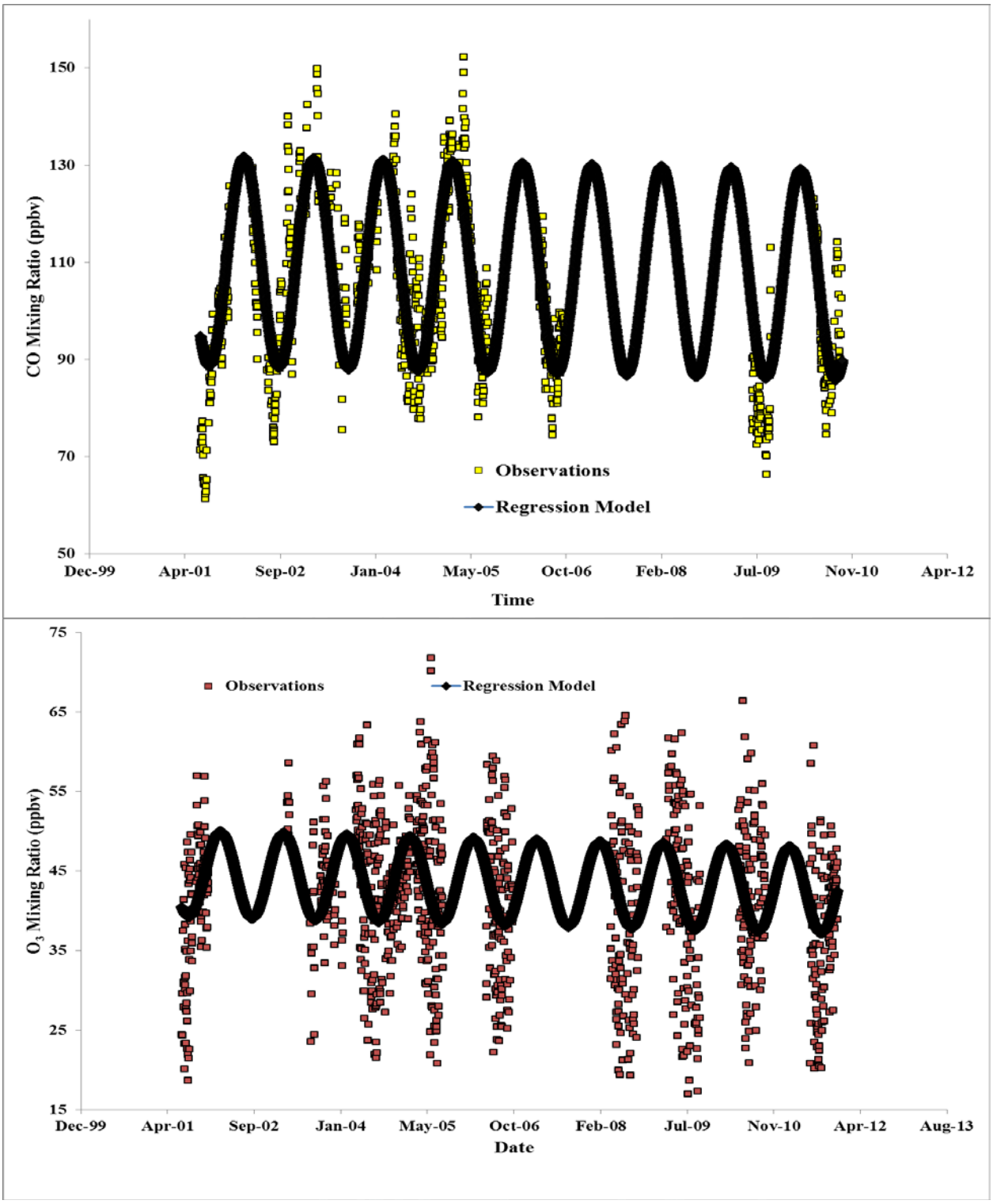

Figure 5. Regression model fit to the PMO observations for CO (top) and O_3 (bottom)

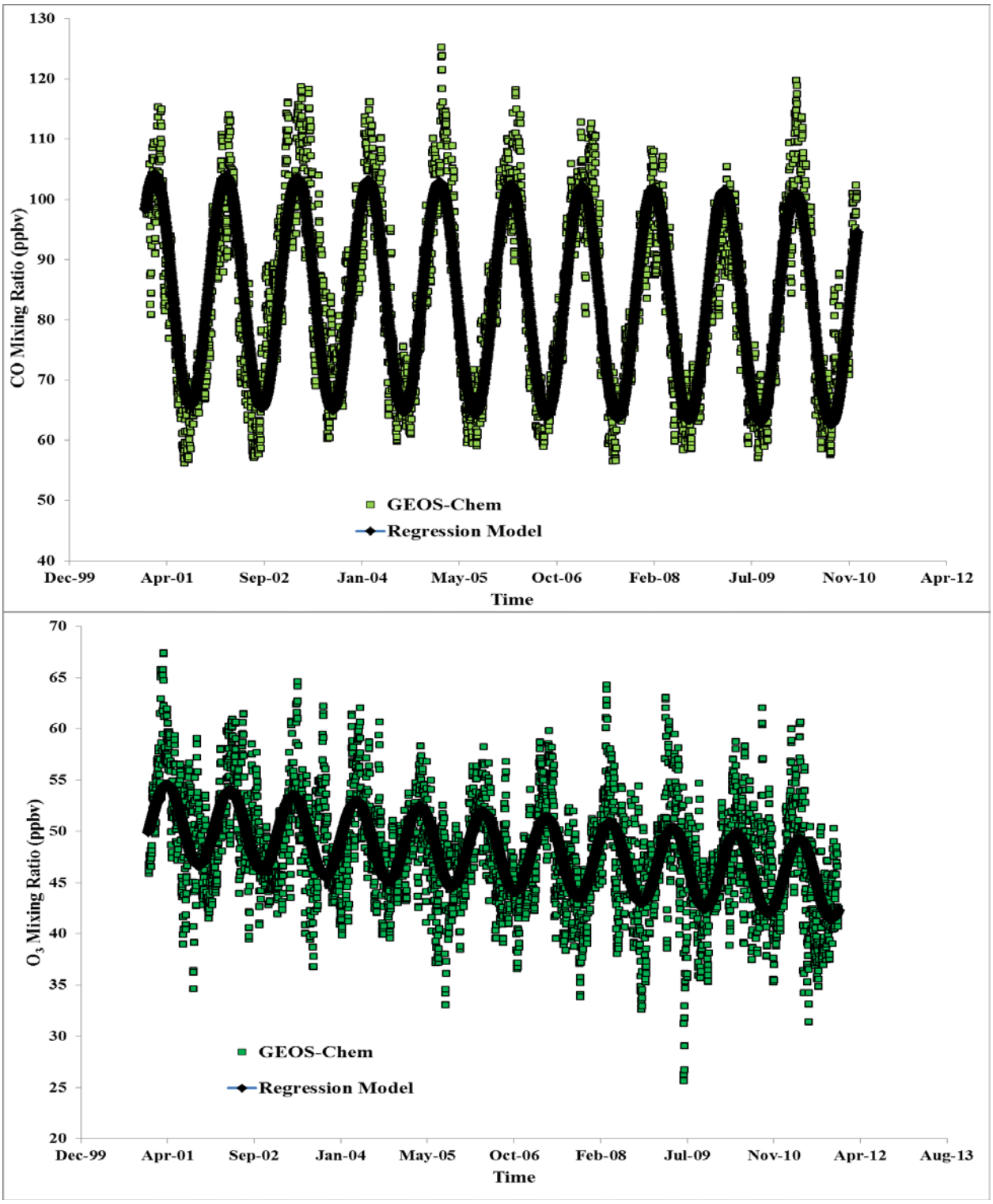

Figure 6. Regression model fit to the GEOS-Chem (full chemistry simulation with normal emissions) output for CO (top) and O_3 (bottom) at PMO